


Received November 5, 2020, accepted November 15, 2020, date of publication November 18, 2020,  
date of current version December 9, 2020.

Digital Object Identifier 10.1109/ACCESS.2020.3038895

# Artificial Neural Network-Based Method for Identifying Under-Inflated Tire in Indirect TPMS

XIAOPING WANG<sup>1</sup>, ZHIWEN CHEN<sup>1,2</sup> , (Member, IEEE), WAN CAO<sup>3</sup>, GUOLIANG XU<sup>2</sup>, LI LIU<sup>4</sup>, SHENG LIU<sup>2</sup>, (Fellow, IEEE), HONGLANG LI<sup>5</sup>, (Senior Member, IEEE), XUNQING SHI<sup>6</sup>, QINGLIN SONG<sup>7</sup>, ZHIYI XIAO<sup>8</sup>, AND CHAO SUN<sup>2</sup>

<sup>1</sup>School of Mechanical Science and Engineering, Huazhong University of Science and Technology, Wuhan 430074, China

<sup>2</sup>Institute of Technological Science, Wuhan University, Wuhan 430072, China

<sup>3</sup>Wuhan FineMEMS Incorporation, Wuhan 430075, China

<sup>4</sup>School of Materials Science and Engineering, Wuhan University of Technology, Wuhan 430070, China

<sup>5</sup>Institute of Acoustics, Chinese Academy of Sciences, Beijing 100190, China

<sup>6</sup>Hong Kong Applied Science and Technology Research Institute Company Ltd., Hong Kong

<sup>7</sup>Goertek Microelectronic Company, Shandong 261031, China

<sup>8</sup>Huatian Technology (Kunshan) Electronics Company Ltd., Jiangsu 215300, China

Corresponding authors: Zhiwen Chen (zwenchen\_lu@163.com) and Sheng Liu (victor\_liu63@vip.126.com)

This work was supported in part by the National Natural Science Foundation of China under Grant 61904127 and Grant 62004144; in part by the Fundamental Research Funds for the Central Universities (young researchers) under Grant 2042019kf0013; in part by the Fundamental Research Funds for the Central Universities under Grant 2042019kf1002, Grant 202401002, and Grant 203134004; in part by the Natural Science Foundation of Hubei Province under Grant 2018CFB212; in part by the Hubei Provincial Natural Science Foundation of China under Grant 2020CFA032; and in part by the Hubei Provincial Major Program of Technological Innovation under Grant 2017AAA121.


**ABSTRACT** Tire pressure monitoring is essential to driving safety. Indirect tire pressure monitoring system (TPMS) is a cost-effective alternative to direct tire pressure monitoring system. Its performance depends on the algorithm for data pre-processing and analysis which is normally complicated, sensitive to initial calibration with limited working range. In this work, four tests were carried out with Baojun 530 with a different deflated tire in each case. Speed data read through ABS CAN bus was analyzed and traditional frequency based method was employed to identify the deflated tire. To simplify the data pre-processing and improve response speed and working range, a new artificial neural network (ANN) based method was also proposed to identify deflated tire based on speed data point collected through antilock brake system (ABS) sensors in tests. A long short-term memory (LSTM) network was developed to locate the deflated tire with an accuracy of 0.83 after training for individual data points. And performance of this method can be further improved by employing a soft voting mechanism with 3 LSTM networks. In proposed ANN based method, benchmark data from properly inflated tire is not required, which makes it a promising solution for multiple deflated tires cases which is challenging for traditional frequency-based method.

**INDEX TERMS** Artificial neural network, tire pressure, indirect tire pressure monitoring system, under-inflated tire.

## I. INTRODUCTION

Tire pressure is essential for driving performance, fuel efficiency and safety of the driver. Low tire pressure can increase the possibility of a car crash that needs braking, because it can lead to longer braking distance. Based on a study from US DoT (Department of Transportation), 27% of passenger cars and 33% of light trucks are operated with one or more substantially under-pressured tire [1]. According to Society

of Automotive Engineering (SAE) report, 260 thousand traffic accidents were caused by tire failure, 75% of which was a result of pressure loss [2]. Hence, tire pressure monitoring system (TPMS) becomes mandatory parts in automobiles in major developed countries (such as US, EU) and developing countries (such as China) [3]. Generally, there are three types of TPMS, direct TPMS (that monitors the status of tires directly by pressure sensor), indirect TPMS (that warns the tire pressure drop by processing signals from sources other than the pressure of tire, such as wheel speed) and hybrid TPMS (both pressure sensor and indirect TPMS are

The associate editor coordinating the review of this manuscript and approving it for publication was Aysegül Ucar .

integrated in one system to overcome situations that indirect TPMS cannot identify) [4]. Though direct TPMS is more reliable in terms of measuring tire pressure, it can be of high cost due to the fact that sensors need to be installed in each tire directly along with wireless communication system to transmit measurement results to a receiver connected to electronic control unit (ECU) [5]. Power supply for sensors in direct TPMS poses another significant issue in service life of sensor and its necessary maintenance [6]. In contrast, indirect TPMS can collect necessary data with existing sensors and ECUs, which can achieve much lower cost and flexible installation.

For indirect TPMS, the common practice is to gain the wheel speed data based on signal from anti-lock braking system (ABS) and build a certain algorithm to analyze the status of tires, thus send warnings if tires are under-inflated [4], [7]. Frequency-based method is frequently employed to evaluate the pressure loss [5], [8], [9]. But it is well known that this method requires several steps of sophisticated data pre-processing (such as wheel speed correction to minimize errors from manufacturing tolerance of gear teeth in data preparation) and complicated method to analyze frequency-based signals. And it is extremely challenging for these algorithms if two tires at the same axle deflates or all the four tires are under-deflated.

In recent years, artificial intelligence has been proved to be powerful in solving classification, prediction and several other types of problems. There are only a few works reporting the application of artificial intelligence in indirect TPMS system. Hemanth M. Praveen *et al.* reported a cloud-based system to classify the tire condition of front axle of heavy duty vehicles for large fleet operators with different vehicle models. The primary output is good or bad regarding the monitored tire condition [10]. Alex Kost trained recurrent neural network-long short-term memory (RNN-LSTM) network and a convolutional neural network (CNN) by simulated data for TPMS to classify the status of tire pressure as under inflation, nominal condition and over inflation [11]. Artificial intelligence has also been adopted to investigated other issues in automotive. A joint time series modelling (JTSM) method based on LSTM and RNN has been proposed by Yang Xing and Chen Lv *et al.* for energy consumption analysis of vehicles, motion prediction of leading vehicle in connected autonomous vehicles and dynamic estimation of the brake pressure of EVs [12]–[14]. Deep RNN model is also commonly used in driver activities recognition [15].

To simplify the data processing and improve response speed and working range of traditional algorithm in indirect TPMS, ANN method was employed to identify the deflated tire among others in this work. Four types of tests were carried out on passenger car. Long short-term memory (LSTM) network was developed and optimized to locate the deflated tire based on speed data from tests. Its classification accuracy was further improved by employing a soft voting mechanism consisted of 3 LSTM networks.

**TABLE 1. Status of each tire in Four experiment tests.**

	Left Front Tire (LF)	Right Front Tire (RF)	Left Rear Tire (LR)	Right Rear Tire (RR)
Test 1	Deflated	Properly inflated	Properly inflated	Properly inflated
Test 2	Properly inflated	Deflated	Properly inflated	Properly inflated
Test 3	Properly inflated	Properly inflated	Properly inflated	Deflated
Test 4	Properly inflated	Properly inflated	Properly inflated	Properly inflated

## II. EXPERIMENTS

Experiments were carried out with Baojun 530 produced by Shanghai General Motors Wuling (SGMW). Four types of tests started by intentionally deflating one tire for each case, including left front tire (LF), right front tire (RF), right rear tire (RR) or no deflated tire (None) (listed in Table 1). The pressure of properly inflated tires was 2.3 bar and that of under-inflated tire was 1.7 bar. Speed range of the four tests was 0m/h~73.01km/h, and speed data was read through ABS CAN bus with Vector CANcaseXL in real time. The data acquisition rate of ABS sensor was 100Hz. The raw data from ABS sensor was series of recorded time when a pulse was triggered. Therefore, wheel speed can be estimated by

$$v = \frac{2\pi r}{N_t \Delta t}, \quad (1)$$

where  $r$  is the radius of wheel, which is 0.35m in this work;  $N_t$  is the number of teeth of gear, which is 42 in tested vehicle. Based on Equation (1), speed of all 4 wheels can be derived and used for further analysis.

After tests, 120000 data points were collected for this study (30000 data points from each test). Two different methodologies were employed to identify the deflated tire, traditional frequency based method and ANN based method. Details of frequency based method is reported in reference [9].

Tensorflow was used to build Artificial Neural Network (ANN) for offline data analysis to identify the deflated tire among others. The input speed range for ANN was 0.22km/h~73.01km/h. The methodology is illustrated in Figure 1. A LSTM network was built and tested by 10-fold cross validation scheme, which is widely employed to evaluate robustness of ANN [16]. Under this scheme, the input data was randomly divided into 10 subgroups. During each evaluation, nine of the subgroups (108000 data points) were selected as the training data to build the model, and the rest subgroup (12000 data points) was used for prediction test. Average prediction accuracy from 10-fold cross validation was accepted as the final categorization accuracy of the network. All these analysis, training and predictions were done offline with personal computer.

If prediction accuracy was not acceptable, parameters and structures of LSTM network were optimized with Random-SearchCV tool in sklearn. It can provide information of the best ANN with its outputs and parameters with given conditions. After tried over 300 ANNs the optimum ANN can be found.

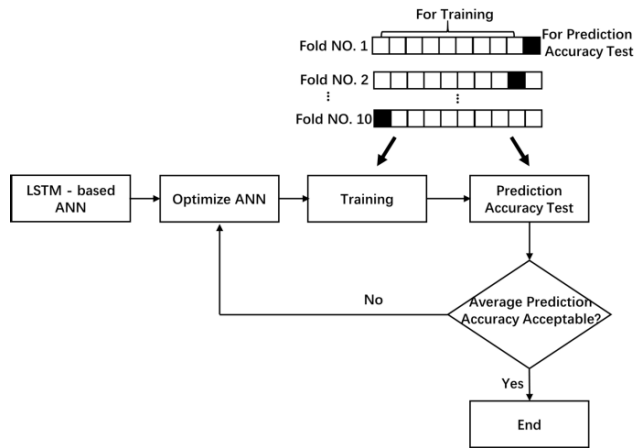


FIGURE 1. ANN-based methodology in this work.

TABLE 2. Details of input data for LSTM network<sup>a</sup>.

Deflated Tire	Label	Number of Data Points	Proportion in Input Data
LF (Test 1)	1	30000	25%
RF (Test 2)	2	30000	25%
LR	3	-	-
RR (Test 3)	4	30000	25%
None (Test 4)	5	30000	25%

<sup>a</sup>Structure of input data: [speed of LF tire, speed of RF tire, speed of LR tire, speed of RR tire, label of data]

Details of input data used in categorization are listed in Table 2. It was consisted of two parts, speed data of each tire and label of the tests, taking the form [speed of LF tire, speed of RF tire, speed of LR tire, speed of RR tire, label of data]. Before feeding to neural network, all nulls in input data were removed and the speed data were then standardized (z-score) in pre-processing. Number of data from different categories are generally the same to guarantee a balance distribution among different categories.

In training, categorical cross-entropy was used as the loss function to estimate the error of LSTM network. The equation is as following [17].

$$CE = - \sum_{c=1}^M t_{o,c} \log(p_{o,c}), \quad (2)$$

where  $M$  is the number of classes,  $t$  is the indicator if class label  $c$  is the correct classification for observation  $o$ ,  $p$  is the predicted probability that observation  $o$  is of class  $c$ .

Softmax was used as the activation function in the output layer of network. This function is widely used in multiclass classification problem. The equation is as following [18].

$$S_i = \frac{e^{V_i}}{\sum_1^n e^{V_j}} \text{ and } \sum_i S_i = 1, \quad (3)$$

where  $V_i$  and  $V_j$  are the  $i_{th}$  and  $j_{th}$  element of the input vector. So, the output for any element will be in the interval (0,1), and all the outputs add up to 1. With input data, softmax function can generate a multiclass probability distribution. The label

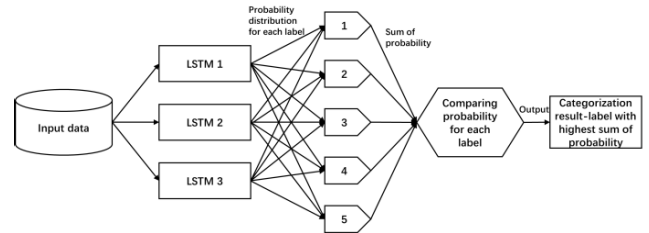


FIGURE 2. Soft voting mechanism for classification.

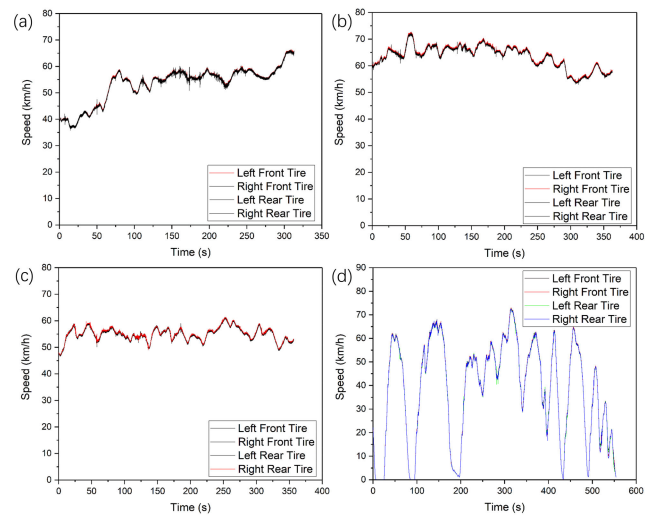


FIGURE 3. Speed spectrum of four wheels in four tests, (a) test 1: left front tire deflated, (b) test 2: right front tire deflated, (c) test 3: right rear tire deflated and (d) test 4: all the four tires are properly inflated.

with highest possibility can be accepted as the categorization result of LSTM network.

To improve the performance of classification, a soft voting mechanism based on LSTM networks was also built. In soft voting, each LSTM provides a probability that a specific data point belongs to a particular target class. Then the label with the greatest sum of probabilities wins the vote. The process of soft voting mechanism is illustrated in Figure 2. For given input data, each of the three LSTM networks would give a probability distribution for the 5 categories (label 1,2,3,4,5). Label with the highest sum of probability will be the final output of this voting LSTM network. This voting mechanism can improve the robustness of ANN and maximize the effect of classifications with relatively higher probability. 10-fold cross validation scheme was also utilized to evaluate the accuracy and robustness of proposed LSTM voting mechanism.

### III. RESULTS

#### A. TEST RESULTS AND FREQUENCY-BASED METHOD

Figure 3 shows the summary of speed spectrum of four wheels in four different tests. It can be found that the speed covered 0-72.9km/h. The wide speed range in test 4 was designed to test the effect of different speed distribution on categorization accuracy.

Figure 4 illustrates the speed difference between deflated tire and the other three properly inflated tires. The speed

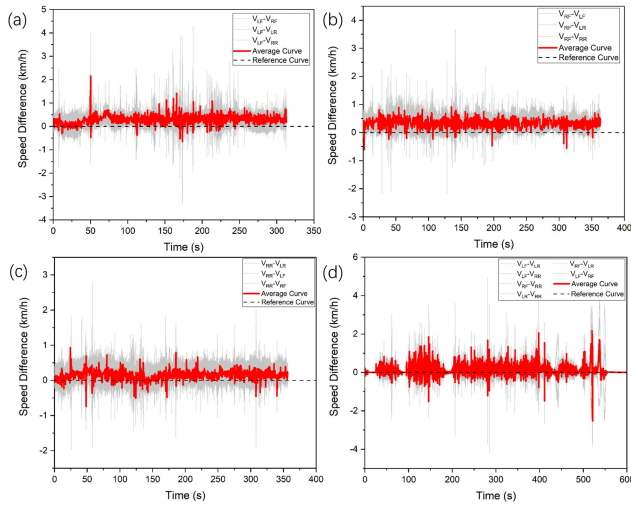


**FIGURE 4.** Speed difference between deflated tire and normal tires in four tests: (a) test 1: left front tire deflated, (b) test 2: right front tire deflated, (c) test 3: right rear tire deflated and (d) test 4: all the four tires are properly inflated.

difference was defined as  $V_{difference} = V_{deflated\ tire} - V_{inflated\ tire}$ . It can be found that the majority of speed difference is slightly higher than 0 km/h in Figure 4 a), b) and c), which means that speed of deflated tire is higher than those of inflated tire. This can be further confirmed by average speed difference (the red curve), which was calculated by  $V_{average\ difference} = (V_{difference1} + V_{difference2} + V_{difference3})/3$ . All the average speed difference curves are higher than 0 km/h. Spikes below the reference curve could be a result of steering condition or sudden change in road conditions. In contrast, in Figure 4 d), both  $V_{difference}$  and  $V_{average\ difference}$  curves are generally symmetry with 0 km/h line in the center. This is consistent with the reports that decreased pressure can lead to drop in effective rolling radius, and thus the deflated tire would rotate faster [8]. Hence, speed of deflated tire is higher than that of properly inflated tire.

After four tests, raw data recorded by sensor was further analyzed according to the methodology described in reference [9]. The natural frequency of inflated tire and deflated tire were analyzed, and the benchmark data was from test 4 with no tires deflated. It was found that the peaks of deflated tire in PSD spectrum was generally lower than those of inflated tires. Figure 5 b) presents an example of different PSD spectrum by frequency-based method based on data from test 1. Analysis results are summarized in Table 3. It can be found that within the tests, a difference of 0.7 to 2.6 can be identified between peaks in PSD spectrum for inflated tire and under-inflated tire. This shows that frequency-based method can be used to identify the under-inflated tire among others.

But several potential drawbacks of this frequency based method were also identified in analysis:

(a) Based on our work, the reported frequency based method works much better at relatively higher speed range, for example above 60km/h in our work. For tests with speed

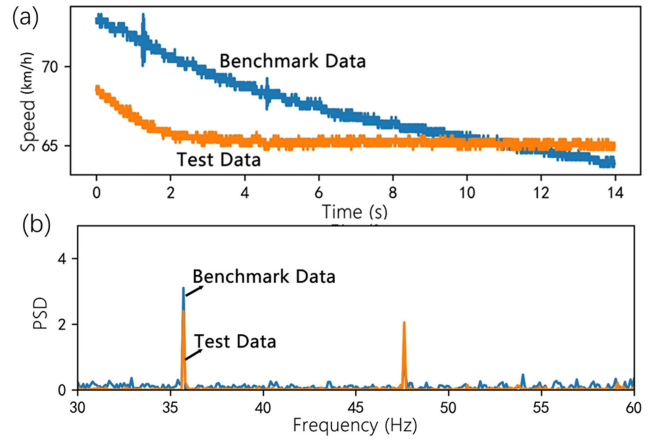


**FIGURE 5.** Example of (a) speed data and (b) PSD spectrum derived from raw data with frequency based method.

**TABLE 3.** Variation among PSD peaks in each test.

Deflated Tire	Differences in Peaks
Test 1	0.7
Test 2	2.6
Test 3	1.2
Test 4	-

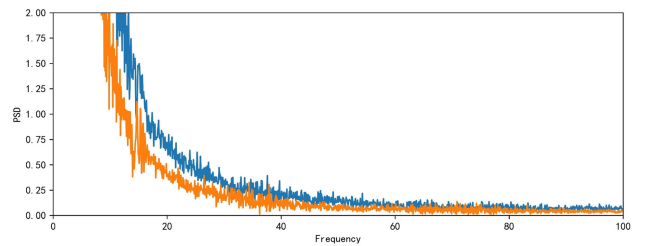


**FIGURE 6.** Example of PSD spectrum from tests with speed range lower than 50km/h.

lower than 40km/h, no noticeable peaks can be identified in PSD spectrum, as illustrated in Figure 6;

(b) In reported frequency-based method, speed data from tests with four properly inflated tire is mandatory to identify tire pressure loss. This set of data serves as a standard for each tire in tests. And complicated data pre-processing is required to extract necessary signal data for identifying under-inflated tire.

(c) One of basic prerequisites for frequency-based method is that the wheel speed will change if tire pressure drops. Though this is true in most cases, it will fail if two tires at the same axle deflate or all the four tires are under-deflated, which can lead to failure of frequency-based method.

**B. PREDICTION ACCURACY OF LSTM NETWORK**

To simplify data pre-processing and improve the performance, LSTM network was built to identify the deflated tire among others based on speed data from ABS sensor. The optimum structure and parameters found in this work (named as LSTM 1) are listed in Table 4. The network consisted of



TABLE 4. Structure of LSTM 1 in this work.

Layer Type	Number of Neurons	Activation Function	
1st Layer (hidden layer)	Dense	10	Relu
2nd Layer (hidden layer)	LSTM	40	Tanh
3rd Layer (hidden layer)	LSTM	30	Tanh
Output Layer	Dense	6	Softmax

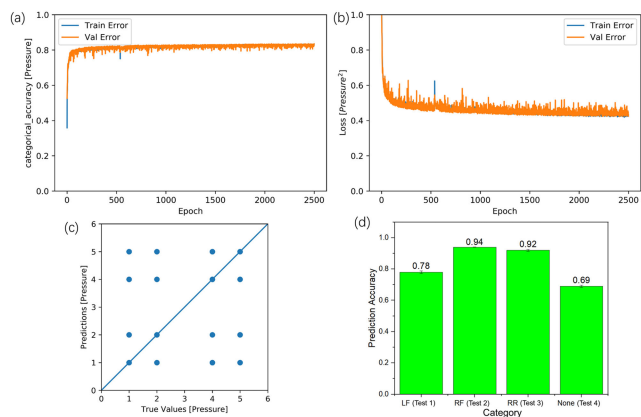


FIGURE 7. Categorization accuracy of LSTM 1 in training and prediction accuracy test: (a) Categorical accuracy in training and validation; (b) Loss in training and validation; (c) Comparison between prediction and true values in prediction accuracy test; (d) Prediction accuracy for each category with error bars.

four layers, input layer, 1st Dense layer, 2nd LSTM layer, 3rd LSTM layer and a Dense layer for output. Adam optimizer with a learning rate of 0.002 was used for ANN optimization. Categorical cross-entropy was used as the loss function, and performance of ANN was evaluated by categorical accuracy.

Figure 7 shows typical evolution of accuracy of LSTM 1 in training and prediction accuracy test. In training, the accuracy increased gradually and plateaued at 0.83 while the loss dropped continuously (Figure 7 a and b). With the trained LSTM network, 19958 out of 24000 data points were categorized correctly in prediction accuracy test. Figure 7(c) and d) illustrate details of prediction accuracy in each category. It shows that the highest accuracy of 0.94 for test 2 and lowest accuracy of 0.69 for test 4. In 10-fold cross validation, it was found that the average prediction accuracy was 0.83 with a deviation of 0.003.

C. PERFORMANCE OF LSTM VOTING MECHANISM

In order to improve the classification accuracy, three of best LSTM networks (LSTM 1, LSTM 2 and LSTM 3) among built networks in this work were employed to form a voting mechanism as described in section II. Details and performance of the three networks were listed in Table 5.

With the same set of training and test dataset as those in section B, the prediction accuracy of this voting mechanism

TABLE 5. Details of LSTM 2 and LSTM 3 employed in soft voting mechanism.

Details of the Network	Prediction Accuracy
LSTM 2 1st hidden layer: Dense, 10 neurons, Relu 2nd hidden layer: LSTM, 40 neurons, Tanh 3rd hidden layer: LSTM, 20 neurons, Tanh 4th hidden layer: Dense, 6 neurons, Softmax	0.82
LSTM 3 1st hidden layer: Dense, 10 neurons, Relu 2nd hidden layer: LSTM, 40 neurons, Tanh 3rd hidden layer: LSTM, 25 neurons, Tanh 4th hidden layer: Dense, 6 neurons, Softmax	0.82

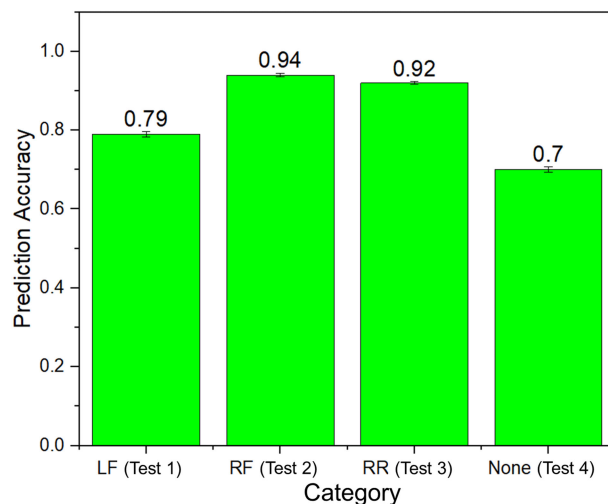


FIGURE 8. Prediction accuracy for each category with error bars by soft voting mechanism.

is 0.84 with deviation of 0.004 in 10-fold cross validation. Detailed accuracy distribution among the 5 categories is illustrated in Figure 8. With soft voting mechanism, the highest prediction accuracy was 0.94 for test 2 and the lowest was 0.7 for test 4. In comparison to LSTM 1, it can be found that prediction accuracy can be slightly improved with the soft voting mechanism. Particularly, the classification accuracy of label 1 and 5 was 0.01 higher than those in Figure 7 d).

IV. DISCUSSION

A. COMPARISON BETWEEN FREQUENCY-BASED METHOD AND ANN

In FMVSS 138, both direct TPMS and indirect TPMS are required to warn the driver within 10 minutes if any tire is under-inflation. In traditional algorithm for indirect TPMS, identification of under inflated tire is normally based on analysis on frequency signal, in which spectrum for a certain duration is required [9]. For proposed ANN method in this work, classification can be done for individual speed data. This means alarms can be given promptly if tire pressure drop happens, because speed data can be fed by ABS speed sensor with high frequency (100Hz in this work).

It should also be noticed that start speed for ANN identification (0.22km/h in this work) can be much lower than traditional indirect TPMS (50km/h in FMVSS 138). This means that ANN based method is capable to identify the

deflated tire before the speed gets too high, which can significantly improve driving safety. On the other hand, complex preprocess of input data is mandatory in traditional frequency based methodology, such as eliminating manufacturing error in ABS tooth ring, wheel speed averaging and filtering. All these data preprocessing is not necessary in ANN based method, which can make the ANN more easily to be deployed in application.

These advantages make ANN potentially more accurate with timely response in applications in comparison to current frequency-based method in indirect TPMS. And driving safety can be further improved. In real application of ANN method, an appropriate time threshold may be needed before giving an alarm. Without this, because ANN processes input data at an individual data point base, the driver could be repeatedly alarmed because of sudden tire speed change (or pressure drop) or sensor malfunction for very short time in an unusually dynamic situation (such as running on a road with poor condition).

In real applications, there are also some potential limitations of proposed ANN method. Setting up ANN model and followed training and validation were done on personal computer with Tensorflow in this work. But, the deployment of built ANN model into ECUs can be challenging in application, because there are some libraries involved in setting up ANN. To achieve this, noticeable work may be required to transfer a complex ANN model into normal mathematics, such as matrix computations. Another potential issue is that performance of ANN (such as prediction accuracy and response speed) is generally dependent on computation capability of hardware and complexity of ANN model. A balance between accuracy and response speed of ANN may be required to deliver the best performance with given ECU capabilities.

## B. POSSIBLE FACTORS THAT LOWER THE PERFORMANCE OF ANN

In both Figure 7d) and Figure 8, the overall performance of ANN was generally limited by the much lower categorization accuracy for data from test 1 and test 4. On the other hand, the categorization accuracy for data from test 2 and test 3 is much higher. One of the possible factors is the imbalanced distribution of speed data. As illustrated in Figure 3, the range of collected data from test 1 and test 4 is notably wider than those from test 2 and test 3. Therefore, the data distribution from the former two tests is more decentralized, which is particularly true for test 4 (as listed in Table 6). This may pose significant negative effect on LSTM training due to much more outliers.

## V. CONCLUSION

In this work, we presented an ANN based methodology to identify the deflated tire among properly inflated tires. Analysis flow and identification accuracy were elucidated. Based on presented results and discussions, following conclusions can be drawn:

**TABLE 6. Major statistics of speed distribution in four tests (km/h).**

	Test 1	Test 2	Test 3	Test 4
Range	36.5~66.5	53.5~72.3	46.9~61.4	0~72.9
Mean	53.6	63.5	55.0	36.7
Standard Deviation	6.7	4.2	2.5	21.2

1. Deflated tire can rotate faster than properly inflated tires and the difference can be identified in PSD spectrum by traditional frequency based method with some drawbacks.
2. In this work, the optimum prediction accuracy of LSTM network is 0.83, and the performance of current ANN is mainly hindered by the decentralized distribution of data.
3. Categorization accuracy of LSTM network can be improved with a soft voting mechanism.
4. ANN based method can identify the deflated tire starting from a much lower speed with more timely response than that requested in FMVSS 138, which makes it capable to provide much better safety.

In future, the performance of ANN will be improved by extending its capability in handling decentralized speed data from ABS to achieve better prediction accuracy without bringing too much extra workload to ECUs. On the other hand, cases with more complicated conditions will be systematically studied by ANN-based method, including two deflated tires, three deflated tires and four deflated tires, which are particularly challenging for traditional frequency-based method. So that, the viability, advantages and potential risks of ANN in TPMS application can be evaluated. After that, we will try to implement this methodology to a vehicle to achieve real-time output with online data collection in our next stage.

## REFERENCES

- [1] S. B. J. P. Schmitz, "Method and apparatus for scavenging and using energy caused by changes in pressure," U.S. Patent 7178389 B2, Dec. 17, 2004.
- [2] L. Yi, L. Qingxia, L. Sheng, and D. Tianlin, "Direct tire pressure monitoring system based on wireless sensor and CAN bus," *Chin. J. Sci. Instrum.*, vol. 29, no. 4, p. 711, 2008.
- [3] B. Fleming, "Tire pressure-monitoring systems rollout," *IEEE Veh. Technol. Mag.*, vol. 4, no. 3, pp. 6–10, Sep. 2009.
- [4] S. Velupillai and L. Guvenc, "Tire pressure monitoring," *IEEE Control Syst. Mag.*, vol. 27, no. 6, pp. 22–25, Dec. 2007.
- [5] S. Solmaz, "A novel method for indirect estimation of tire pressure," *J. Dyn. Syst., Meas., Control*, vol. 138, no. 5, May 2016, Art. no. 054501.
- [6] Y. Leng, Q. Li, B. Hou, S. Liu, and T. Dong, "Wheel antenna of wireless sensors in automotive tire pressure monitoring system," in *Proc. Int. Conf. Wireless Commun., Netw. Mobile Comput.*, Shanghai, China, Sep. 2007, pp. 2755–2758.
- [7] Q. Zhang, B. Liu, and G. Liu, "Design of tire pressure monitoring system based on resonance frequency method," in *Proc. IEEE/ASME Int. Conf. Adv. Intell. Mechatronics*, Singapore, Jul. 2009, pp. 781–785.
- [8] N. Persson, F. Gustafsson, and M. Drevö, "Indirect tire pressure monitoring using sensor fusion," *SAE Int.*, vol. 111, pp. 1657–1662, Jan. 2002.
- [9] J. Zhao, J. Su, B. Zhu, and J. Shan, "An indirect TPMS algorithm based on tire resonance frequency estimated by AR model," *SAE Int. J. Passenger Cars Mech. Syst.*, vol. 9, no. 1, pp. 99–106, Apr. 2016.

[10] O. Svensson, S. Thelin, S. Byttner, and Y. Fan, "Indirect tire monitoring system—machine learning approach," *IOP Conf. Series, Mater. Sci. Eng.*, vol. 252, Oct. 2017, Art. no. 012018.

[11] A. Kost, "Applying neural networks for tire pressure monitoring systems," M.S. thesis, Dept. Mech. Eng., California Polytech. State Univ., San Luis Obispo, CA, USA, 2018.

[12] Y. Xing, C. Lv, and D. Cao, "Personalized vehicle trajectory prediction based on joint time-series modeling for connected vehicles," *IEEE Trans. Veh. Technol.*, vol. 69, no. 2, pp. 1341–1352, Feb. 2020.

[13] Y. Xing and C. Lv, "Dynamic state estimation for the advanced brake system of electric vehicles by using deep recurrent neural networks," *IEEE Trans. Ind. Electron.*, vol. 67, no. 11, pp. 9536–9547, Nov. 2020.

[14] Y. Xing, C. Lv, D. Cao, and C. Lu, "Energy oriented driving behavior analysis and personalized prediction of vehicle states with joint time series modeling," *Appl. Energy*, vol. 261, Mar. 2020, Art. no. 114471.

[15] Y. Xing, C. Lv, H. Wang, D. Cao, E. Velenis, and F.-Y. Wang, "Driver activity recognition for intelligent vehicles: A deep learning approach," *IEEE Trans. Veh. Technol.*, vol. 68, no. 6, pp. 5379–5390, Jun. 2019.

[16] H. Zhang, S. Yang, L. Guo, Y. Zhao, F. Shao, and F. Chen, "Comparisons of isomiR patterns and classification performance using the rank-based MANOVA and 10-fold cross-validation," *Gene*, vol. 569, no. 1, pp. 21–26, Sep. 2015.

[17] S. Marsland, "The Multi-layer Preception," in *Machine Learning: An Algorithmic Perspective*, 2nd ed. Boca Raton, FL, USA: CRC Press, 2011, p. 81.

[18] S. Raschka and V. Mirjalili, "Parallelizing neural network training with TensorFlow," in *Python Machine Learning: Machine Learning and Deep Learning With Python, Scikit-Learn, and TensorFlow*, 2nd ed. Birmingham, UK: Packt, 2019, p. 446.



**XIAOPING WANG** was born in Xiangfan, Hubei, China, in 1978. He received the M.S. degree from the Wuhan University of Technology. He is currently pursuing the Ph.D. degree in engineering with the Huazhong University of Science and Technology.

From December 2000 to November 2002, he worked with Wuhan Telecom Device Company, as a Project Manager. From November 2002 to July 2003, he worked with Wuhan Kedi Optical Communication Company Ltd., as a Project Manager. He was a Project Manager, a System Manager, and the Dean of the Research Institute with Shanghai FineMEMS Company Ltd., from August 2003 to June 2009. From July 2009 to December 2017, he worked with Shanghai FineMEMS Company Ltd., as a Deputy General Manager. Since January 2018, he has been a General Manager with Wuhan FineMEMS Company Ltd. In 2018, he won the first prize of the Chinese Academy of Electronics Technology Invention Award as the second author. He has filed or granted more than 20 patents and authored five technical articles on MEMS sensors and system products.



**ZHIWEN CHEN** (Member, IEEE) was born in Hubei, China, in 1987. He received the bachelor's degree from the Huazhong University of Science and Technology and the Ph.D. degree from the Wolfson School of Mechanical, Electrical and Manufacturing Engineering, Loughborough University, U.K.

After graduation, he joined the Institute of Technological Science, Wuhan University, as an Associate Professor. He has published 16 technical articles and filed/granted more three patents. His research interest includes mechanics in electronic packaging and modeling.



**WAN CAO** was born in Wuhan, Hubei, China in 1981. He received the B.S. degree major in computer network from the Wuhan University of Technology.

He is proficient in computer programming, digital circuit and single-chip computer programming, and familiar with the software and hardware architecture of the Internet. He worked with Shanghai FineMEMS Company Ltd., from July 2005 to September 2012, and worked as a Research and Development System Engineer and a Project Manager for tire pressure project and pressure sensor project. Since September 2012, he has been with Wuhan FineMEMS Company Ltd. He is currently a Manager of the Research and Development Department, responsible for research and development. He has filed or granted more than 20 patents and authored two technical articles on MEMS sensors and system products.

**GUOLIANG XU**, photograph and biography not available at the time of publication.

**LI LIU**, photograph and biography not available at the time of publication.

**SHENG LIU**, photograph and biography not available at the time of publication.

**HONGLANG LI**, photograph and biography not available at the time of publication.

**XUNQING SHI**, photograph and biography not available at the time of publication.

**QINGLIN SONG**, photograph and biography not available at the time of publication.

**ZHIYI XIAO**, photograph and biography not available at the time of publication.

**CHAO SUN**, photograph and biography not available at the time of publication.

...